

# Fast-Degradable Microbeads Encapsulating Human Umbilical Cord Stem Cells in Alginate for Muscle Tissue Engineering

Jun Liu, D.D.S., Ph.D.,<sup>1,2</sup> Hongzhi Zhou, D.D.S., Ph.D.,<sup>1</sup> Michael D. Weir, Ph.D.,<sup>1</sup> Hockin H.K. Xu, Ph.D.,<sup>1,3-5</sup> Qianming Chen, D.D.S., Ph.D.,<sup>2</sup> and Carroll Ann Trotman, B.D.S., M.A., M.S.<sup>6,7</sup>

Human umbilical cord mesenchymal stem cells (hUCMSCs) are inexhaustible and can be obtained without an invasive surgery. To date, there has been no report on seeding hUCMSCs in three-dimensional scaffolds for muscle tissue engineering. The objectives of this study were to (1) investigate hUCMSC seeding in a scaffold for muscle engineering and (2) develop a novel construct consisting of hUCMSC-encapsulating and fast-degradable microbeads inside a hydrogel matrix. The rationale was that the hydrogel matrix would maintain the defect volume, while the microbeads would degrade to release the cells and concomitantly create macropores in the matrix. hUCMSCs were encapsulated in alginate-fibrin microbeads, which were packed in an Arg-Gly-Asp (RGD)-modified alginate matrix (AM). This construct is referred to as hUCMSC-microbead-AM. The control consisted of the usual cell encapsulation in AM without microbeads (referred to as hUCMSC-AM). In the hUCMSC-AM construct, the hUCMSCs showed as round dots with no spreading at 1–14 days. In contrast, cells in the hUCMSC-microbead-AM construct had a healthy spreading and elongated morphology. The microbeads successfully degraded and released the cells at 8 days. Myogenic expressions for hUCMSC-microbead-AM were more than threefold those of hUCMSC-AM ( $p < 0.05$ ). Immunofluorescence for myogenic markers was much stronger for hUCMSC-microbead-AM than hUCMSC-AM. Muscle creatine kinase of hUCMSC-microbead-AM at 14 days was twofold that of hUCMSC-AM ( $p < 0.05$ ). In conclusion, hUCMSC encapsulation in novel fast-degradable microbeads inside a hydrogel matrix was investigated for muscle engineering. Compared to the usual method of seeding cells in a hydrogel matrix, hUCMSC-microbead-AM construct had greatly improved cell viability and myogenic differentiation, and hence, is promising to enhance muscle regeneration.

## Introduction

MUSCULAR DISEASES (e.g., muscular dystrophy), congenital defects (e.g., cleft lip), and defects due to trauma and tumor-ablative surgery often cause significant loss of muscle tissue. The supply of muscle tissues to treat large muscle defects remains a major challenge. Muscle tissue engineering with the use of stem cells and scaffolds is a promising approach to solving this problem.<sup>1-4</sup> Autologous muscle satellite cells located in mature muscles and indicated as a heterogeneous population of committed myogenic and uncommitted progen-

itors have been used for muscle regeneration<sup>3,5</sup>; however, obtaining these cells is invasive and their purification is difficult. Moreover, these cells have a relatively low expansion capability with limited quantity, and these factors are problematic for the repair of large muscle defects.<sup>6</sup> Mesenchymal stem cells (MSCs) are promising for tissue engineering and have been harvested from a number of tissues, including bone marrow, adipose, and umbilical cord tissues. Efforts have been made to use bone marrow MSCs in muscle engineering.<sup>7</sup>

Human umbilical cords can be obtained without additional invasive procedures. Recently, the Wharton's jelly of

<sup>1</sup>Biomaterials and Tissue Engineering Division, Department of Endodontics, Prosthodontics and Operative Dentistry, University of Maryland Dental School, Baltimore, Maryland.

<sup>2</sup>State Key Laboratory of Oral Diseases, West China School of Stomatology, Sichuan University, Chengdu, China.

<sup>3</sup>Center for Stem Cell Biology and Regenerative Medicine, University of Maryland School of Medicine, Baltimore, Maryland.

<sup>4</sup>University of Maryland Marlene and Stewart Greenebaum Cancer Center, University of Maryland School of Medicine, Baltimore, Maryland.

<sup>5</sup>Department of Mechanical Engineering, University of Maryland, Baltimore County, Maryland.

<sup>6</sup>University of Maryland Dental School, Baltimore, Maryland.

<sup>7</sup>School of Dentistry, University of North Carolina, Chapel Hill, North Carolina.

umbilical cords was identified as a promising source of MSCs.<sup>8,9</sup> Several investigations have used human umbilical cord MSCs (hUCMSCs) for tissue engineering of bone and cartilage.<sup>10–13</sup> Only a few studies investigated hUCMSCs for muscle engineering by culturing on dishes, or injecting into animals.<sup>14–16</sup> To date, there has been no report on using a three-dimensional scaffold to seed hUCMSCs for myogenic differentiation.

Scaffolds are another key component for tissue engineering.<sup>17,18</sup> Several types of scaffolds have been used to support growth and differentiation of progenitor cells for muscle engineering, including natural scaffolds such as alginate,<sup>19–21</sup> fibrin, and collagen,<sup>22,23</sup> as well as synthetic scaffolds.<sup>3,24–26</sup> Hill *et al.* used alginate scaffolds with macropores fabricated by orthodontic wires for cell seeding. Their approach led to a higher cell viability and efficient migration of myoblasts when compared to nanoporous and microporous alginate scaffolds.<sup>19</sup> In some applications, it is desirable to have fast-degradable hydrogel microbeads with stem cell encapsulation. The microbeads could be mixed into an injectable paste that is placed into a defect, and the paste sets or polymerizes to maintain the tissue shape. Then, the microbeads could quickly degrade to release the cells throughout the matrix, while concomitantly creating macropores. Alginate hydrogels take weeks or months to degrade. However, novel oxidized alginate-fibrin microbeads encapsulating hUCMSCs were recently developed that could degrade and release the cells at 4 days.<sup>27</sup> These fast-degradable microbeads were packed inside a calcium phosphate cement in which the microbeads quickly degraded and released the hUCMSCs with good viability.<sup>28</sup> Literature search revealed no report on cell-encapsulating alginate-fibrin microbeads incorporation in a hydrogel matrix.

Therefore, the objective of this study was to develop a construct consisting of fast-degradable microbeads inside a slow-degradable hydrogel matrix with hUCMSC delivery for muscle engineering. It was hypothesized that, compared to the usual method of directly encapsulating cells in a hydrogel matrix, the novel hUCMSC-encapsulating fast-degradable microbeads packed in the hydrogel matrix would yield much better hUCMSC viability and greatly enhanced myogenic differentiation.

## Materials and Methods

### Materials

Sodium alginate (UP LVG; ProNova) was purchased from FMC. G<sub>4</sub>RGDSP (Gly<sub>4</sub>-Arg-Gly-Asp-Ser-Pro) peptides were purchased from Peptides International. 1-Ethyl-3-[3-dimethylaminopropyl] carbodiimide hydrochloride (EDC), N-hydroxysulfosuccinimide (sulfo-NHS), 2-(N-morpholino)ethanesulfonic acid (MES), and Slide-A-Lyzer dialysis cassette kit with 3.5K molecular-weight cutoff (MWCO) were from Thermo Fisher. The low-glucose Dulbecco's modified Eagle's medium (DMEM), the high-glucose DMEM, the calcium-free DMEM, MSC-qualified fetal bovine serum (FBS), horse serum (HS), penicillin-streptomycin-glutamine, Dulbecco's phosphate-buffered saline (D-PBS), and trypsin were purchased from Invitrogen. Chick embryo extract (CEE) was from Accurate. Monoclonal mouse antibody against MyoD (clone MoAb 5.8A) and myogenin (clone F5D) were purchased from BD Pharmingen. Monoclonal

mouse antibody against myosin heavy chain (MYH; clone A4.1025) was from Millipore and antibody against sarcomeric  $\alpha$ -actinin (ACTN; clone EA-53) from Sigma-Aldrich. Goat anti-mouse Alexa Fluor 488 IgG and Alexa Fluor 594 IgG were from Molecular Probes, Invitrogen. 4',6-diamino-2-phenylindole (DAPI) was from Millipore. All other chemicals were from Sigma-Aldrich.

### Cell culture and myogenic induction

hUCMSCs were from ScienCell, which were harvested from the Wharton's Jelly in umbilical cords of healthy babies. The use of hUCMSCs was approved by the University of Maryland. The growth medium was composed of low-glucose DMEM supplemented with 1% penicillin-streptomycin-glutamine and 10% of MSC-qualified FBS. Passage 5 cells were used. For myogenic culture, two types of media were used: the myogenic inductive medium, and the myogenic proliferative medium. The myogenic inductive medium consisted of high-glucose DMEM, 20% FBS, 1% penicillin-streptomycin-glutamine, and 10  $\mu$ M 5-azacytidine (5-Aza).<sup>14,29,30</sup> The myogenic proliferative medium had high-glucose DMEM, 20% FBS, 1% penicillin-streptomycin-glutamine, 10% HS, and 1% CEE. Both 5-Aza and HS are myogenic supplements.<sup>14,29,30</sup> Following the established methods,<sup>14</sup> hUCMSCs were cultured in the myogenic inductive medium for 2 days and then cultured in the myogenic proliferative medium. As detailed in previous studies, the myogenic proliferative medium was used after 2 days with HS to continue to induce myogenesis.<sup>14,29</sup> The medium was changed every 3 days.

### Arg-Gly-Asp (RGD)-modified and oxidized alginate

Alginate was modified with covalently conjugated oligopeptides as described previously.<sup>19,20,31,32</sup> Lyophilized alginate was added to the MES buffer (0.1M, pH 6.5, containing 0.3M NaCl) to yield 50 mL of 1% (w/v) solution. Then EDC (50 mmol/mol uronic acid), Sulfo-NHS (25 mmol/mol uronic acid), and an RGD sequence-containing peptide (G<sub>4</sub>RGDSP; 3.4 mmol/mol uronic acid, that is, 13 mg/g alginate) were added.<sup>19,32</sup> The solution was stirred for 20 h, and then hydroxylamine (69.5 mg/g alginate) was added to stop the reaction. After dialyzing with ddH<sub>2</sub>O for 3 days, the solution was further purified with activated charcoal (0.5 g/g alginate). This yielded Arg-Gly-Asp (RGD)-modified alginate which was filtered, lyophilized, and stored at  $-20^{\circ}\text{C}$ .

Alginate was partially oxidized to increase its degradability.<sup>32</sup> The sugar residues in alginate were oxidized by reacting with sodium periodate with the production of hydrolytically labile bonds in the polysaccharide.<sup>32</sup> The percentage of oxidation (%) was the number of oxidized uronate residues per 100 uronate units in the alginate chain. Alginate of up to 5% oxidation was previously synthesized.<sup>33</sup> In our recent studies,<sup>27,28</sup> alginate at 7.5% oxidation was synthesized to further increase its degradability. Sodium periodate was added into 1% (w/v) alginate in dd H<sub>2</sub>O. The reaction was performed in a dark room for 24 h and then stopped using an excess of ethylene glycol (1 g/g alginate). The solution was washed with ethanol, collected by centrifugation (Eppendorf Centrifuge 5804; Eppendorf) at 4200 rcf, and redissolved in ddH<sub>2</sub>O. Then, the oxidized alginate solution was lyophilized and stored at  $-20^{\circ}\text{C}$ .<sup>27,28</sup> The 7.5% oxidized alginate was used to fabricate the microbeads.

### Fabrication of hUCMSC-encapsulating hydrogel constructs

Two types of constructs were developed. In the first, hUCMSCs were encapsulated in RGD-modified alginate matrix (AM). This is referred to as hUCMSC-AM, with AM referring to the RGD-modified AM. This construct is schematically shown in Figure 1A. This is the usual method of encapsulating cells in a hydrogel, and its fabrication followed previous procedures.<sup>19,34</sup> Two percent (w/v) alginate solution was made by dissolving the RGD-modified alginate in a calcium-free DMEM and then sterile filtered. The alginate solution containing hUCMSCs was filled in a disk mold of 6.4-mm diameter and 2-mm thickness. The hUCMSC seeding density was  $10^6$  cells per mL of alginate solution, following previous studies.<sup>11,27</sup> This solution was gelled by adding 2 M calcium chloride ( $\text{CaCl}_2$ ) at a ratio of 5  $\mu\text{L}$  of  $\text{CaCl}_2$  per 64  $\mu\text{L}$  of alginate solution. The resulting hUCMSC-encapsulating disk was washed with the low-glucose DMEM and cultured as described in the following sections.

The second type consisted of hUCMSC-encapsulation in fast-degradable microbeads, which were then packed in AM. To make the oxidized alginate-fibrin microbeads, fibrinogen

from bovine plasma (Sigma-Aldrich) was added into the 7.5%-oxidized alginate in the calcium-free DMEM and incubated at 37°C for 2 h. A fibrinogen concentration of 0.1% was selected following a previous study.<sup>27</sup> hUCMSCs were added at  $10^6$  cells per mL of the solution. The cross-linking solution was prepared using a 100-mM  $\text{CaCl}_2$  solution in distilled water containing 1 unit/mL of thrombin (Sigma-Aldrich). The microbeads were formed by extruding the alginate-fibrinogen droplets into the cross-linking solution using a bead-generating device (Var J1; Nisco). This produced hUCMSC-encapsulating microbeads of approximately 200–300  $\mu\text{m}$  in sizes.<sup>27</sup>

The microbeads were added into the RGD-modified alginate solution, with the microbeads as the fillers and the RGD-modified alginate as the matrix. This composite solution was filled in a disk mold of 6.4-mm diameter and 2-mm thickness to make disks. The microbead volume fraction in the disk was 20%; this is referred to as hUCMSC-microbead-AM, and schematically shown in Figure 1B. It should be noted that the AM contained RGD, but the microbeads did not contain RGD. This is because the preliminary experiment showed that adding RGD in microbeads retained the cells in the microbeads and hindered the cell release from the microbeads.

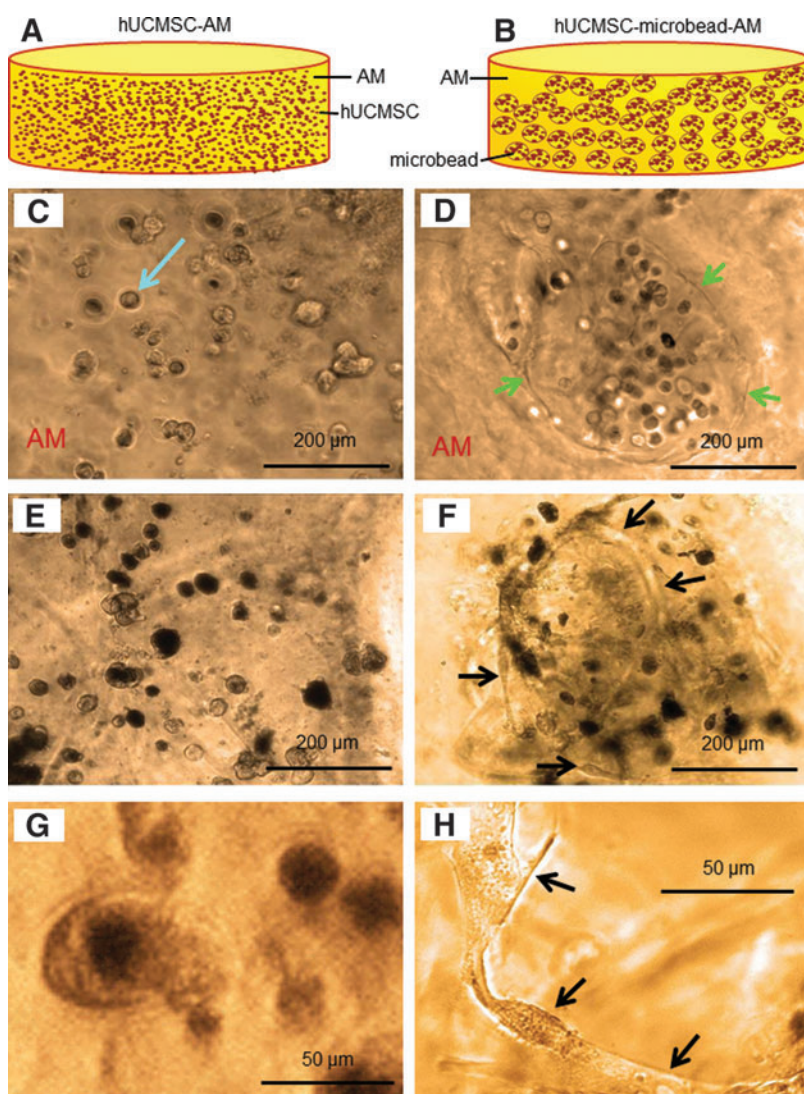


**FIG. 1.** (A) Schematic of Arg-Gly-Asp (RGD)-modified alginate encapsulating human umbilical cord mesenchymal stem cells (hUCMSCs) (referred to as hUCMSC-AM, AM = RGD-modified alginate matrix). (B) hUCMSCs in degradable alginate-fibrin microbeads in AM (referred to as hUCMSC-microbead-AM). Optical photos of hUCMSC-AM (C, E, G) and hUCMSC-microbead-AM (D, F, H). At 1 day, cells were round-shaped in (C) and (D). Arrow in (C) indicates a cell. Arrows in (D) indicate the microbead boundary. Such microbead boundary disappeared due to microbead degradation at 8 days. At 14 days, cells remained as dots in (E), but become elongated in (F). (G) and (H) Higher magnification shows round cells in hUCMSC-AM, and elongated and spreading cells in hUCMSC-microbead-AM at 8 days. Color images available online at [www.liebertpub.com/tea](http://www.liebertpub.com/tea)



### Cell viability

After the constructs were cultured in the growth medium for 1, 3, 7, and 14 days, cell viability was determined with a live/dead viability kit (Invitrogen). The samples were incubated with ethidium homodimer (4  $\mu$ M) and calcein-AM (2  $\mu$ M) for 2 h at 37°C. Cells were then observed via epifluorescence microscopy (Eclipse TE2000-S; Nikon). Live cells were stained green and dead cells were stained red. Four randomly taken fluorescence images for each sample were analyzed, with five samples ( $n=5$ ), yielding 20 images for each time point. The percentage of live cells = Number of live cells / (live cells + dead cells).<sup>10</sup> In addition, the spreading of the live cells was quantified. The maximal diameters of the live cells in the images were measured using ImageJ software (version 1.44p; NIH). This was measured from the images of the five samples for each construct type at each time point.

To measure cell viability, the constructs were treated with 3-(4,5-dimethylthiazol-2-yl)-2, 5-diphenyltetrazolium bromide (MTT). After adding the MTT solution, the encapsulated cells were incubated for 5 h in an incubator at 37°C with 5% CO<sub>2</sub>, during which purple formazan crystals were formed. The medium was removed carefully, then the hydrogel was homogenized and the formazan crystals were extracted by adding 0.5 mL of dimethyl sulfoxide. After the mixture was incubated for 40 min, the solution was transferred into 96-well plates, and the absorbance was measured at 570 nm using a SpectraMax M5 microplate reader (Molecular Devices). The MTT absorbance was obtained at 1, 3, 7, and 14 days, and normalized to the absorbance of the same type of constructs measured at 1 day.

### Reverse transcription-polymerase chain reaction analysis of myogenic differentiation

To collect the cells, the alginate gels were depolymerized using 55 mM sodium citrate and the 0.15 M sodium chloride buffer at 37°C for 30 min, as previously described.<sup>35</sup> Then, the cells were recovered following 10 min of centrifugation at 260 rcf and washed with D-PBS. A minimum of  $1 \times 10^5$  cells were thus prepared, lysed in TRIzol reagent (Invitrogen), and stored at -80°C. The total RNA was purified using the PureLink RNA Mini Kit (Invitrogen), and the quantity and purity of isolated RNA were analyzed using a Nanodrop 2000 spectrophotometer (Thermo Scientific). The total RNA was reverse transcribed into cDNA on a GeneAmp PCR System 2700 (Applied Biosystems). The real-time polymerase chain reactions (PCRs) were carried out in the Applied Biosystems 7900HT Real-Time PCR with TaqMan Fast Universal PCR Master Mix, No AmpErase UNG. The TaqMan Gene Expression Assays Hs00153812\_m1, Hs00947164\_g1, and Hs99999901\_s1 were used for  $\alpha$ -actinin 3 (*ACTN3*), *myosin heavy chain 1* (*MYH1*), and *18S ribosomal RNA* (*18S*), respectively. The data were analyzed using RQ Manager (version 1.2.1; Applied Biosystems) according to the  $2^{-\Delta\Delta Ct}$  method. Relative target mRNA expression levels were normalized against the housekeeping gene *18S*. All the groups were calibrated to the type 1 samples cultured in the growth medium under equivalent conditions at 0 day.

### Immunofluorescence analysis of myogenic markers

Cell encapsulating hydrogels were washed with low-glucose DMEM, hardened using 50 mM CaCl<sub>2</sub>,<sup>36</sup> and fixed

and permeabilized in cold methanol.<sup>37</sup> Then, the hydrogels were incubated in the low-glucose DMEM buffer for 1 h to block the nonspecific binding. The samples were incubated overnight with primary antibodies (including MyoD, myogenin, ACTN, and MYH; 1:100) in the DMEM buffer containing 5% FBS and then washed with DMEM for three times. The hydrogels were then incubated with goat anti-mouse Alexa Fluor 488 IgG or Alexa Fluor 594 IgG (1:200 in 5% FBS/DMEM) for 4 h. Samples were counterstained with DAPI (0.5  $\mu$ g/mL in DMEM) for 10 min to visualize nuclei. The primary antibodies were omitted for negative controls. Cells were examined via a Nikon Eclipse TE2000-S fluorescence microscopy and photographed using the Nikon DS-Qi1Mc camera and NIS Elements BR software.

Cells were collected by depolymerizing the alginate gel as described above, suspended in growth media, transferred to a tissue culture-treated 48-well plate (Falcon; BD Biosciences), and incubated for 1 h at 37°C to allow for attachment.<sup>38</sup> The cells were permeabilized with 0.1% Triton X-100 in PBS for 10 min after fixation using 4% paraformaldehyde. Nonspecific binding was blocked with 1% bovine serum albumin (BSA) in 0.2% Triton X-100 in PBS (PBT) for 1 h. The primary monoclonal ACTN antibodies in the antibody-blocking buffer were applied at 36.5°C for 1 h. Cells were incubated with goat anti-mouse Alexa Fluor 594 IgG (1:200) in 1% BSA/PBT for 30 min. For nuclear detection, the cells were counterstained with DAPI (0.2  $\mu$ g/mL in PBS) for 1 min.

### Muscle creatine kinase activity

Cells were collected and lysed in 0.5% Triton X-100 (40  $\mu$ L per disk), followed by 2 min of centrifugation at 16,000 rcf at 4°C. The supernatant was saved separately to determine the muscle creatine kinase (MCK) activity and total protein content. Ten microliter supernatant and 200  $\mu$ L of CK-NAC reagent (Fisher) was added to a 96-well plate in duplicate, which was run on a SpectraMax M5 microplate reader (Molecular Devices) at 37°C. Following the manufacturer's instructions,<sup>39</sup> the change in absorbance was measured at 340 nm over 3 min (20 s intervals) and then converted to activity in units per liter (U/L). The MCK activity was normalized with total protein concentration in the sample, which was determined following a previous method.<sup>40,41</sup>

### Scanning electron microscope and statistics

To examine pores in alginate hydrogel matrix, the hydrogels were collected and freeze-dried. The samples were fractured, mounted, sputter-coated with platinum/palladium, and examined with a scanning electron microscope (SEM, Quanta 200; FEI).

One-way and two-way analysis of variance were used to detect significant effects of the variables. Tukey's multiple comparison tests were performed to compare the data and the  $p$ -value  $\leq 0.05$ .

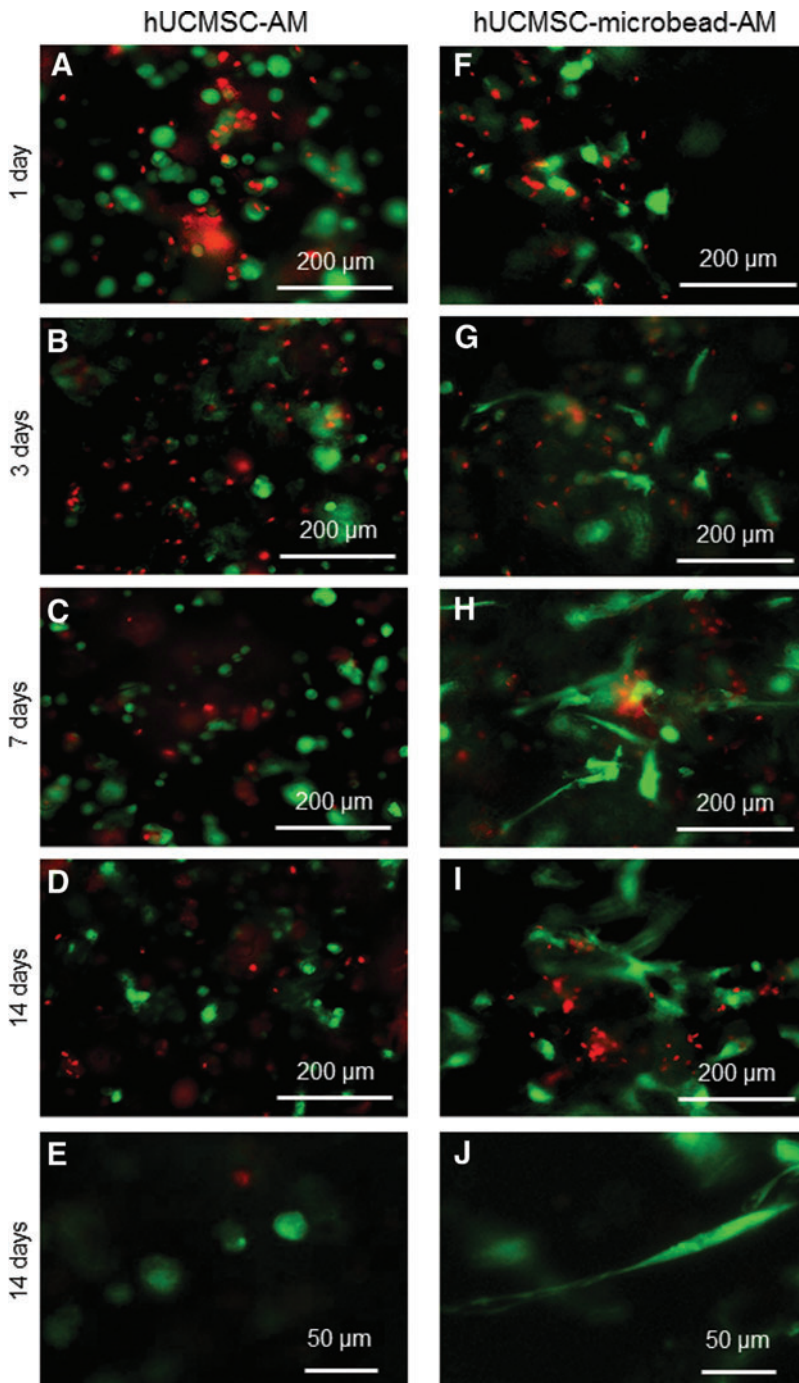
## Results

Figure 1A and B show schematically the two types of constructs. The same cell seeding density of  $10^6$  cells per mL of alginate solution was used in fabricating the hUCMSC-AM construct in Figure 1A and the microbeads in Figure 1B.

In Figure 1A, the hUCMSC-AM construct had cells throughout its volume, with  $6.4 \times 10^4$  cells per disk. In Figure 1B, the hUCMSC-microbead-AM construct had 20% of microbeads, and only the microbeads contained the cells; hence, there were approximately  $1.3 \times 10^4$  cells per disk. From Figure 1C–H, the left column shows hUCMSC-AM, and the right column shows hUCMSC-microbead-AM. In Figure 1C and Figure 1D at 1 day, cells were round with no spreading. Arrows in Figure 1D indicate the boundary of a microbead, embedded in the alginate matrix AM. In Figure 1E at 14 days, hUCMSC-AM still had rounded cells. In contrast, in Figure 1F at 14 days, hUCMSC-microbead-AM had some

rounded cells, and some spreading cells (arrows). Microbead boundary, such as that in Figure 1D at 1 day, was not visible at 8 days and 14 days, indicating microbead degradation. The difference between the two constructs is seen more clearly at a higher magnification, with Figure 1G showing rounded cells in hUCMSC-AM, and Figure 1H showing spreading and elongated cells in hUCMSC-microbead-AM, both at an intermediate time of 8 days.

The difference between the two types of constructs is further demonstrated in the fluorescence images of live (green) and dead (red) cells (Fig. 2). At 1 day, both constructs had live cells appearing as green dots. hUCMSC-AM had



**FIG. 2.** Live/dead staining of cells in hUCMSC-AM (A–E), and in hUCMSC-microbead-AM (F–J). In contrast to live cells being green dots in hUCMSC-AM, live cells in hUCMSC-microbead-AM started to have a spreading morphology in (G). Cells spread better in (H) and (I). (E) and (J) Typical higher magnification views showed cells not spreading in hUCMSC-AM, in contrast to healthy spreading and elongated cells in hUCMSC-microbead-AM. Color images available online at [www.liebertpub.com/tea](http://www.liebertpub.com/tea)

cells with a rounded morphology from 1 to 14 days. In Figure 2G, hUCMSC-microbead-AM started to have cells with a spreading morphology at 3 days. Cells spread better at 7 days (Figure 2H) and 14 days (Figure 2I). At a higher magnification, examples of rounded cells in hUCMSC-AM are shown in Figure 2E. The spreading and elongated cells in hUCMSC-microbead-AM are evident in Figure 2J.

The qualitative differences in cell viability observed in Figure 2 are quantified in Figure 3: Figure 3A, percentage of live cells; Figure 3B, MTT viability; and Figure 3C, cell spreading sizes (mean  $\pm$  sd;  $n=5$ ). At 7 days, the percentage of live cells was  $67\% \pm 5\%$  in hUCMSC-microbead-AM, higher than  $51\% \pm 4\%$  in hUCMSC-AM. Cells in hUCMSC-microbead-AM had higher MTT than hUCMSC-AM ( $p < 0.05$ ). A higher MTT absorbance indicates a higher metabolic activity and higher cell viability. The live cell spreading size (mean  $\pm$  sd;  $n=5$ ) was quantified in Figure 3C. The cells overwhelmingly spread better in hUCMSC-microbead-AM than in hUCMSC-AM at each time period ( $p < 0.05$ ). These results show that the viability of hUCMSCs was enhanced by encapsulation in the fast-degradable microbeads in AM.

Reverse transcription-polymerase chain reaction results were measured to investigate myogenic differentiation (Fig. 4). In (A), the *ACTN3* expression greatly increased over 14 days. *ACTN3* expression for hUCMSC-microbead-AM was 3–5 times higher than that for hUCMSC-AM. In Figure 4B, myogenic marker *MYH1* increased at 2 and 7 days in hUCMSC-AM, and over 14 days in hUCMSC-microbead-AM. Compared to hUCMSC-AM, the *MYH1* expression for hUCMSC-microbead-AM was more than 10 times higher at 2 and 14 days. These results indicate that the hUCMSCs in the fast-degradable microbeads in AM had better myogenic differentiation than the direct cell seeding in AM without microbeads.

In immunofluorescence staining in Figure 5, comparison between Figure 5E and Figure 5A indicates a strong MyoD staining for hUCMSC-microbead-AM, but little staining for hUCMSC-AM on day 7. There was a weak staining for myogenin in hUCMSC-AM in Figure 5B, and strong staining in hUCMSC-microbead-AM in Figure 5F. *ACTN* and *MYH* (red) were also weak in hUCMSC-AM, and strong in hUCMSC-microbead-AM. Cells in hUCMSC-microbead-AM had spreading and started to fuse into multinucleated elements at 14 days. This is more clearly shown in Figure 5I and Figure 5J at a higher magnification, where arrows indicate blue nuclei of multiple cells that appeared to have fused together into a single element. Figure 5K plots the MCK activity, which is an enzyme known to increase during late myogenic differentiation.<sup>42</sup> At 14 days, the MCK of hUCMSC-microbead-AM was twofold that of hUCMSC-AM ( $p < 0.05$ ). These results confirm that the novel hUCMSC-microbead-AM construct enhanced the myogenic differentiation of hUCMSCs.

To understand the reason for the enhanced myogenic differentiation in hUCMSC-microbead-AM, SEM examination of the scaffolds was performed (Fig. 6). hUCMSC-AM had no macropores from 1–14 days, with an example in Figure 6A at 1 day. Microbead degradation created macropores P in hUCMSC-microbead-AM, indicated by arrows in Figure 6B at 7 days, and Figure 6C at 14 days. The macropores in hUCMSC-microbead-AM had sizes of several hundred microns, similar to the starting microbead sizes.

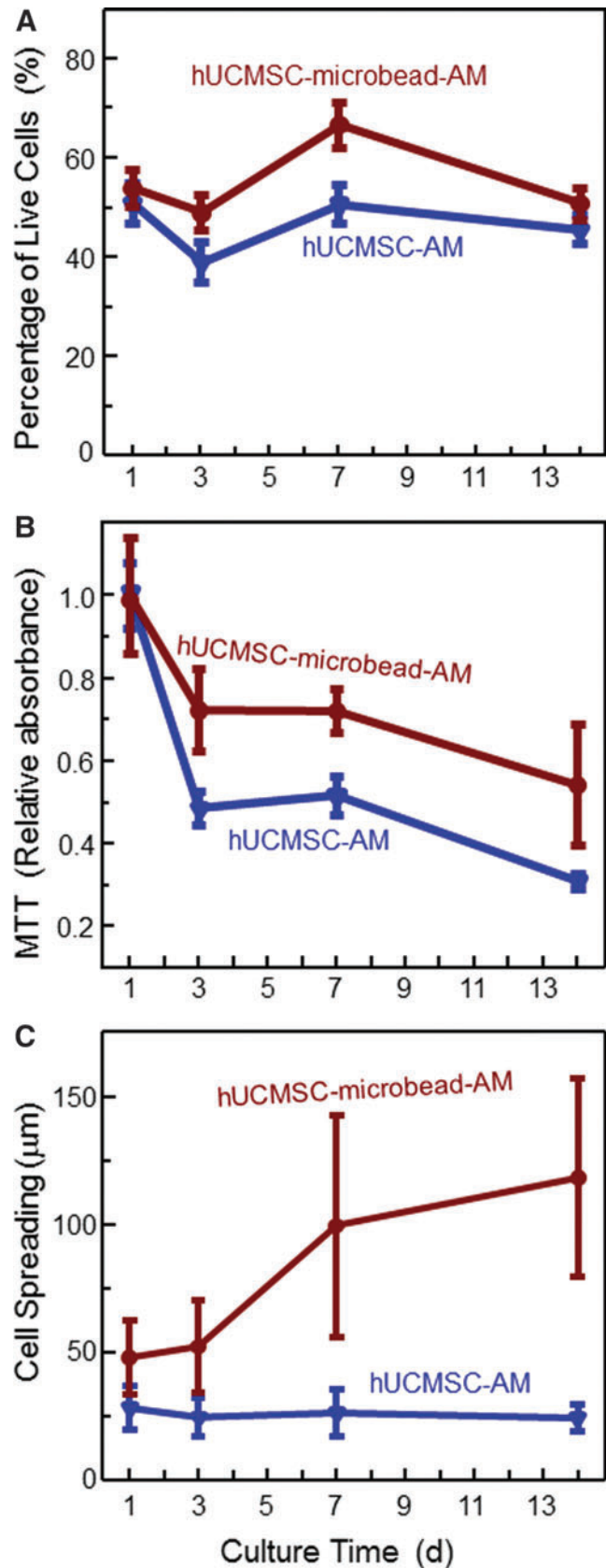


FIG. 3. Viability of the encapsulated hUCMSCs: (A) percentage of live cells, (B) MTT assay of metabolic activity of cells, and (C) cell spreading size. Each value is mean  $\pm$  sd ( $n=5$ ). Color images available online at [www.liebertpub.com/tea](http://www.liebertpub.com/tea)



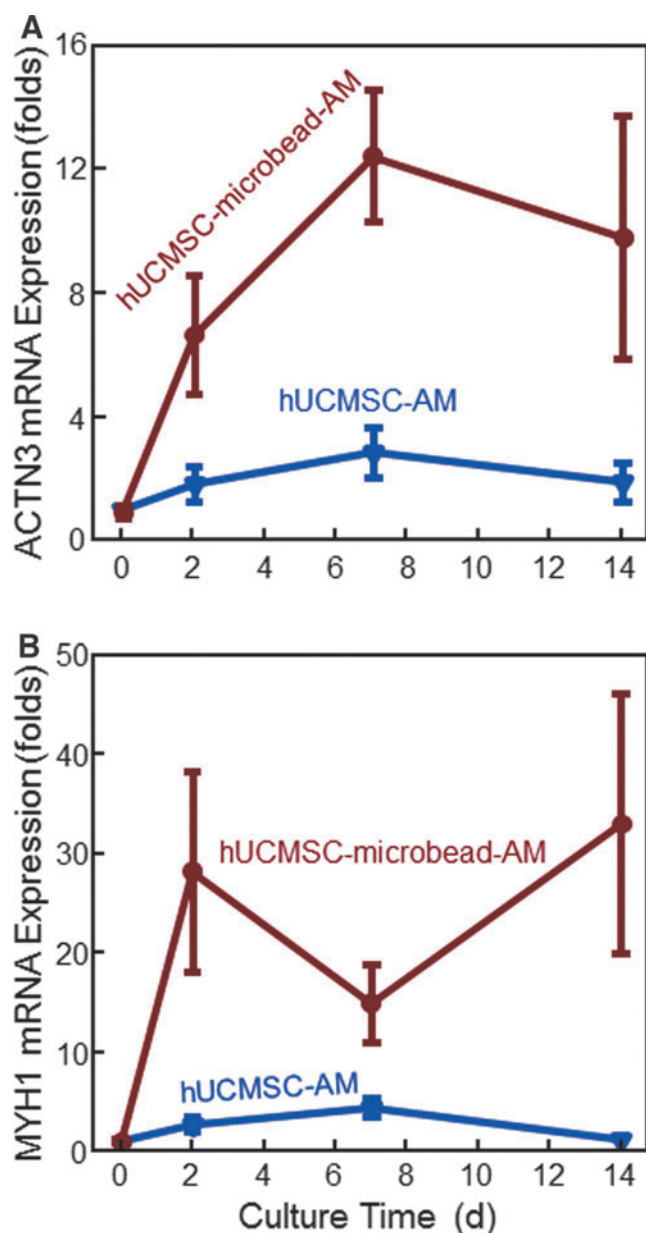


FIG. 4. Reverse transcription-polymerase chain reaction (RT-PCR) analysis of myogenic gene expressions: (A)  $\alpha$ -actinin 3 (*ACTN3*), and (B) *myosin heavy chain 1* (*MYH1*). Each value is mean  $\pm$  sd;  $n=5$ . The new hUCMSC-microbead-AM construct yielded much higher myogenic gene expressions than hUCMSC-AM. Color images available online at [www.liebertpub.com/tea](http://www.liebertpub.com/tea)

## Discussion

Literature search revealed no report on hUCMSC seeding in a three-dimensional scaffold for muscle tissue engineering. Only a few previous studies investigated myogenic differentiation of hUCMSCs by culturing the cells on dishes *in vitro*, or injecting the cells into animals.<sup>14–16</sup> None of these previous studies used any scaffold to seed hUCMSCs for myogenic differentiation.<sup>14–16</sup> In the present study, hUCMSC-encapsulating construct with fast-degradable microbeads in an AM was developed for muscle tissue engineering. The microbeads could degrade and release the cells

throughout the AM, while creating macropores via microbead degradation. After the stem cell-encapsulating construct is implanted, it is beneficial for the cells to be quickly released from the microbeads, so that the cells can spread and attach to the macroporous scaffold to enhance cell function. The present study used fast-degrading microbeads, because a recent study showed that the regular alginate microbeads did not degrade and failed to release the encapsulated cells after 21 days; hence, the cells remained in the microbeads as round dots.<sup>27</sup> The reason that fibrin was added to the microbeads was that even oxidized alginate microbeads failed to release the cells at 14 days; however, the oxidized alginate-fibrin microbeads quickly degraded and released the cells at 4 days.<sup>27</sup> In addition, our preliminary experiments showed that adding RGD in the AM enhanced the attachment and spreading of the released cells. However, adding RGD into the microbeads appeared to keep the cells inside the microbeads and hindered cell release from the microbeads. Therefore, RGD was only incorporated into the AM, but not into the microbeads. The hUCMSC seeding density was  $10^6$  cells/mL of alginate solution, following previous studies<sup>11,27</sup>; future study should investigate the effect of cell density in AM and in microbeads on myogenic differentiation. It should be noted that, while the overall cell seeding density was  $10^6$  cells/mL, upon degradation of the microbeads, more cells appeared to adhere to the surface of the macropores in the scaffold. This likely resulted in a higher local cell density at the pore surface than the distributed cell density in the control scaffold without macropores. Further study should investigate how this higher local cell density affects cell viability, protein secretion, cell–cell interactions, and myogenic differentiation.

The results of a recent study<sup>27</sup> and the preliminary experiments suggested that the lack of macropores in hUCMSC-AM inhibited cell spreading, while the degradation of microbeads in hUCMSC-microbead-AM released the cells and created macropores. This allowed the cells to attach to the RGD-modified macroporous alginate scaffold, which enhanced cell viability. The hUCMSCs in hUCMSC-microbead-AM scaffold successfully differentiated into the myogenic lineage with a well spreading morphology, strong positive immunofluorescence staining for early (*MyoD* and *myogenin*) and late (*ACTN* and *MYH*) myogenic markers, and highly increased *ACTN3* and *MYH1* gene expressions, and the MCK activity. The MCK of a 0.08 U/mg protein for hUCMSC-microbead-AM at 14 days was similar to the MCK activity of mouse primary myoblasts detected previously.<sup>43</sup> At 14 days, the cells started to fuse into multinucleated elements (Fig. 5I, J). Hence, the novel hUCMSC-microbead-AM construct appeared promising for bone tissue engineering applications.

Hydrogel microbeads have the advantage of better nutrient diffusion into the microbeads. Fibrin microbeads may be fabricated by a preheated oil emulsion method.<sup>44</sup> These preformed microbeads could only be used for cell attachment on the surface, but not cell encapsulation inside the microbead.<sup>45</sup> In other studies, relatively large fibrin beads of about 3 mm in diameter were made to encapsulate cells,<sup>46</sup> and fibrin microbeads of 50–300  $\mu$ m in diameter were prefabricated in hot oil and then seeded with cells on the surfaces. In addition, bulk scaffolds of alginate were fabricated,<sup>19</sup> and alginate beads of 3.6-mm and 2.2-mm diameters were made for cell encapsulation. These beads were not

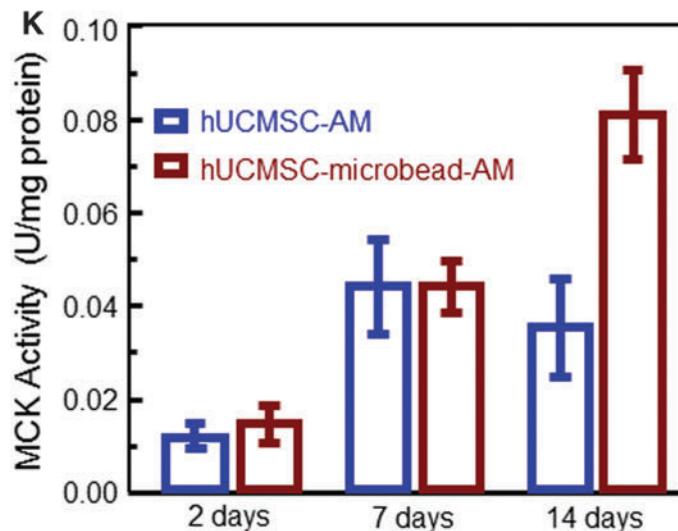
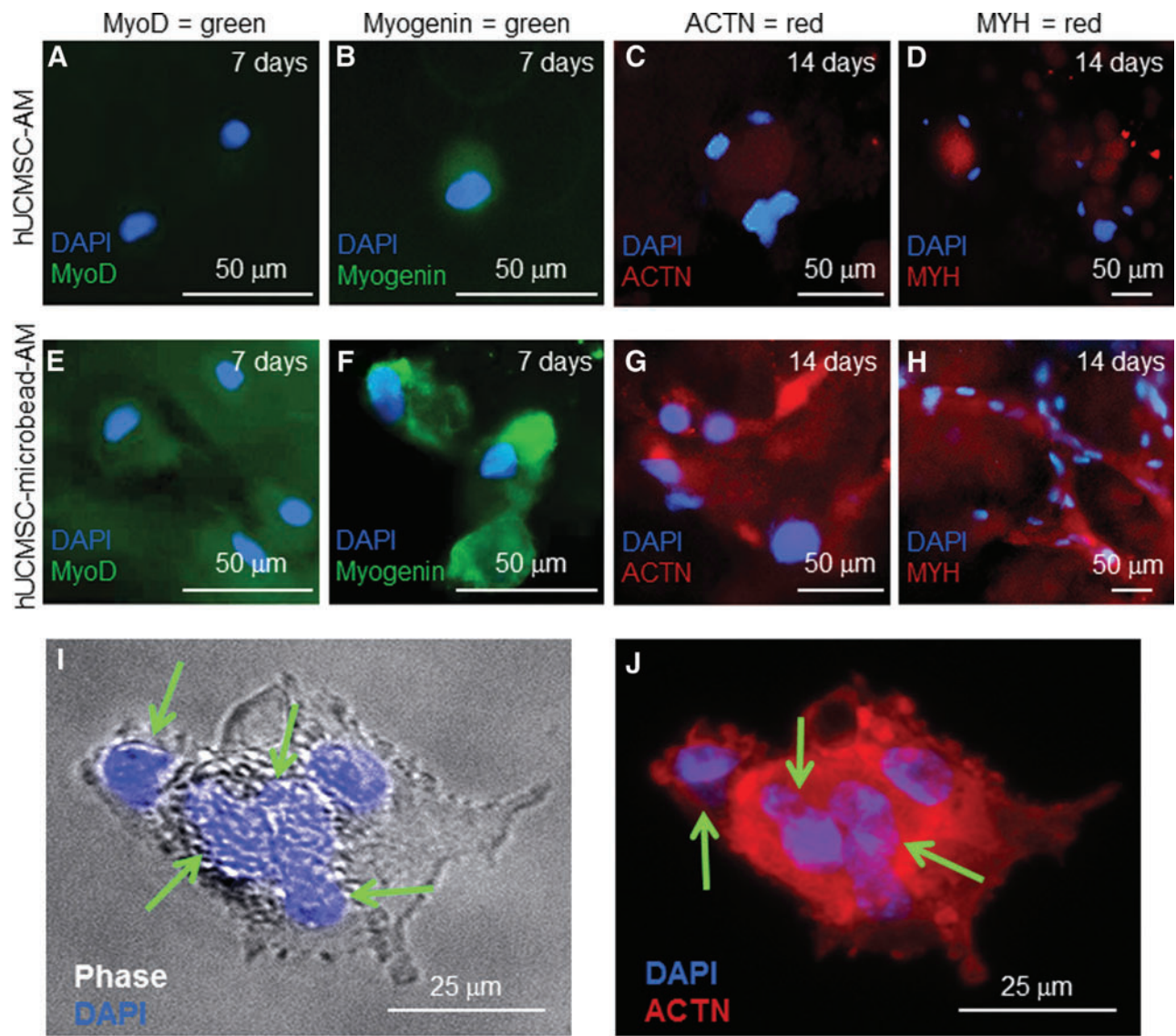


**FIG. 5.** Myogenic differentiation. (A–J) Immunofluorescence images, (K) muscle creatine kinase (MCK) activity. In (A–J), the first row is for hUCMSC-AM, and the second row is for hUCMSC-microbead-AM. MyoD and myogenin, known as early myogenic differentiation markers,<sup>42</sup> were stained at 7 days. Sarcomeric  $\alpha$ -actinin (ACTN) and myosin heavy chain (MYH), known as late myogenic markers,<sup>42</sup> were stained at 14 days. Cells in hUCMSC-AM had a weak staining of MyoD (A, green), myogenin (B, green), ACTN (C, red), and MYH (D, red). In contrast, hUCMSC-microbead-AM had much stronger staining. At 14 days, cells in hUCMSC-microbead-AM had a spreading shape and started to fuse into multinucleated elements (G and H). (I and J) Multinucleated elements of fused cells recovered from hUCMSC-microbead-AM at 14 days. Arrows point to the multiple nuclei. In (K), each value is mean  $\pm$  sd;  $n=5$ . Color images available online at [www.liebertpub.com/tea](http://www.liebertpub.com/tea)



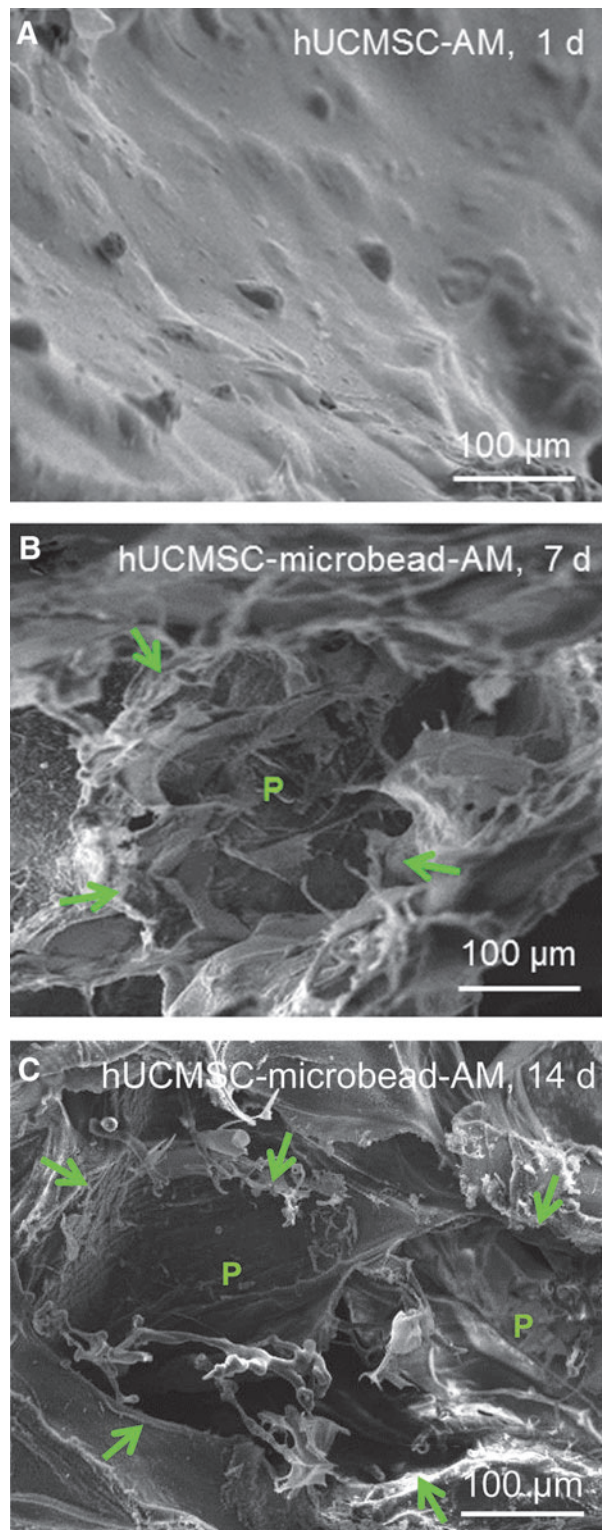


**FIG. 6.** SEM of hydrogel constructs: (A) hUCMSC-AM at 1 day, and (B, C) hUCMSC-microbead-AM at 7 and 14 days, respectively. No macropores were found in hUCMSC-AM from 1 to 14 days, similar to that shown in (A). In (B), the microbead was degraded and macropore P was formed at 7 days. (C) Macropore formed by the degradation of possibly two microbeads at 14 days. The macropores in alginate matrix had sizes of several hundred microns. Arrows in (B) and (C) demonstrate the macropores. Color images available online at [www.liebertpub.com/tea](http://www.liebertpub.com/tea)

shown to degrade and did not release the cells.<sup>47,48</sup> Another study developed RGD-modified alginate microbeads of 1 mm in diameter, but bead degradation and cell release were not mentioned.<sup>49</sup> A recent study fabricated alginate microbeads of approximately 200  $\mu\text{m}$  for cell encapsulation; no microbead degradation or cell release was reported.<sup>10</sup> Therefore, compared to these previous studies, the uniqueness of the present study was that hUCMSCs were encapsulated in alginate-fibrin microbeads with several hundred  $\mu\text{m}$  in size suitable for injection, and the microbeads were then packed into a hydrogel matrix for muscle tissue engineering. This system significantly enhanced cell viability and myogenic differentiation, compared to the usual method of direct cell seeding into a hydrogel.

The enhanced cell function was likely due to the microbead degradation that increased the porosity in the AM. Efforts were made to develop porous scaffolds to enhance cell migration and mass transport.<sup>50–52</sup> Porous alginate scaffolds were fabricated by various methods with a wide range of pore sizes, ranging from nanometer-scale to several hundred microns.<sup>19,24,53</sup> Unmodified alginate had pores of 5–200 nm in diameter.<sup>54</sup> The freeze-drying technique yielded porous alginate with pores of <100  $\mu\text{m}$ .<sup>19,37,55</sup> A gas-foaming process using the reaction between acetic acid and sodium bicarbonate with  $\text{CO}_2$  release was utilized to construct porous alginate.<sup>53</sup> Hill *et al.* used orthodontic wires to create a macroporous scaffold with 400–500- $\mu\text{m}$  pores.<sup>19</sup> Macroporous alginate scaffolds enhanced cell viability and migration.<sup>19</sup> Porous scaffolds are commonly used for cell seeding after scaffold formation, rather than cell encapsulation before scaffold gelation. Hwang *et al.* fabricated porous alginate (150–300- $\mu\text{m}$  pores) using gelatin microspheres as a porogen for generating pores inside cell-laden alginate.<sup>56</sup> Although their method allowed cell encapsulation and pore creation, cells in alginate gel could not move and did not spread. In the present study, the unique alginate-fibrin microbeads allowed cell encapsulation inside an alginate hydrogel matrix before gelation. Fibrin has a porous fibrous structure; hence, adding fibrin likely loosened the alginate structure, yielding more degradable microbeads.<sup>27</sup> Furthermore, fibrin could improve cell attachment and spreading.<sup>57</sup> In the present study, microscopic examinations confirmed the cell spreading inside the alginate-fibrin microbeads. The degradable microbeads released the cells throughout the hydrogel matrix, while creating macropores with sizes of about 200–300  $\mu\text{m}$ . This was manifested by cells developing a spreading and elongated morphology. Furthermore, the increased porosity in hUCMSC-microbead-AM likely contributed to the higher percentage of live cells and the metabolic activity, as well as enhanced myogenic expression, myogenic marker staining, and the MCK activity, compared to the control without microbeads.

The prevention of cell spreading might prevent myogenesis of MSCs; hence, cell spreading is important for myogenic differentiation.<sup>58</sup> This was confirmed by the observation that only spreading MSCs induced the expression of laminin  $\alpha 2$  chain, which played a key role in myogenesis.<sup>59</sup> In the present study, hUCMSCs had a healthy spreading and elongated morphology in hUCMSC-microbead-AM, while cells maintained as dots in hUCMSC-AM. This is consistent with previous studies showing that alginate constructs (with or without RGD modification) had only nm-scale pores and cell spreading was inhibited in alginate.<sup>60</sup> Besides cell

spreading, the percentage of live cells was increased to 67% in hUCMSC-microbead-AM. This percentage of live cells is consistent with, or slightly higher than, the reported 30%–50% of cell viability for myoblasts in alginate.<sup>19</sup> Therefore, the novel approach of hUCMSC-encapsulation in fast-degradable microbeads in AM yielded cell spreading, improved cell viability, and enhanced myogenic differentiation.

In the present study, RGD-modified alginate was used as the hydrogel matrix, and the hUCMSC-encapsulating microbeads could be readily mixed into the RGD-modified alginate. After injection or placement into a tissue site, the RGD-modified alginate can gel to form the matrix, thus forming and maintaining the desired shape and contour for muscle regeneration. Alginate was selected as an encapsulating gel because it is biocompatible and can form a cross-linked gel under mild conditions without significantly harming the cells.<sup>19–21</sup> While the present study used alginate as a model system to investigate hUCMSC delivery and the effects of RGD and microbeads on myogenic differentiation, it should be noted that other systems, such as fibrin,<sup>22</sup> collagen,<sup>23</sup> and synthetic scaffolds,<sup>3,24–26</sup> are also promising for tissue engineering applications. The AM was used because a pile of microbeads without this matrix to bond them together would not be able to maintain the shape and contour of the defect. In addition, this hydrogel matrix is beneficial because bioactive agents, such as RGD, can be incorporated into this matrix to interact with the cells released from the degradable microbeads.<sup>61</sup> Although soluble RGD peptide is related with cell death,<sup>31,62</sup> immobilized RGD peptide is important for cell adhesion,<sup>63–65</sup> migration,<sup>19,66</sup> and differentiation.<sup>37,55</sup> In the present study, when macropores were created within the matrix with the degradation of microbeads, cells were released into the macroporous matrix, thus allowing the RGD-modified AM to help enhance myogenic differentiation. Further studies are needed to investigate the effects of porosity and incorporation of RGD and other bioactive agents on *in vivo* muscle regeneration via the novel hUCMSC-microbead-AM construct in an animal model.

A major impetus for this research is to explore approaches to create muscle tissue for the lip muscle defect in babies born with cleft lip and palate. In these patients, muscle tissue in the area of the cleft lip defect is deficient, and this muscle deficiency can be highly variable ranging from a minor loss to a moderate-severe deficiency. Although the former situation may not be a problem for the surgeon to achieve a satisfactory lip repair, for those patients with a moderate-severe muscle deficiency, the esthetic surgical result may be compromised. For example, after primary lip repair, many patients have a residual impairment in movement and the facial esthetics is compromised.<sup>67–69</sup> The ability to supplement and/or generate tissue in the cleft area may be of significant advantage for both the surgeon and the patient. Moreover, as discussed earlier, the method described here has the potential to be of benefit for many other patients with both congenital and acquired muscle deficiencies and disorders.

## Conclusions

The present study (1) encapsulated hUCMSCs in a three-dimensional scaffold for muscle tissue engineering; and (2) developed a novel cell encapsulation method by pack-

ing fast-degradable cell-encapsulating microbeads into an RGD-modified AM. AM would maintain the shape, while microbeads would quickly degrade and release the cells throughout the matrix and concomitantly create macropores. The new approach greatly improved cell viability and myogenic differentiation, compared to the usual method of encapsulating the cells into the hydrogel matrix without microbeads. hUCMSCs in microbeads in alginate differentiated into the myogenic lineage, with cell elongation, elevated *ACTN3* and *MYH1* gene expressions and MCK activity, strong immunofluorescence staining for myogenic markers (MyoD, myogenin, ACTN, and MYH), and multinucleated elements formation by cell fusion. Compared to hUCMSC-AM control, the new hUCMSC-microbead-AM construct had much higher cell survival, better spreading morphology, and substantially enhanced myogenic expressions through the 14 days observed. The novel hUCMSC-microbead-AM construct may be promising for dental, craniofacial and skeletal muscle engineering applications.

## Acknowledgments

We thank Dr. Wenchuan Chen for fruitful discussions and experimental help, and Dr. Xuedong Zhou of the West China School of Stomatology for support. This study was supported by NIH/NIDCR R01 DE14190 (HX) and R21 DE022625 (HX), R01 DE013814 (CT) and R41 DE01974 (CT), Maryland Stem Cell Fund (HX), Maryland Nano-Biotechnology Award (HX), University of Maryland Dental School, and West China School of Stomatology.

## Disclosure Statement

No competing financial interests exist.

## References

- Mao, J.J., Vunjak-Novakovic, G., Mikos, A.G., and Atala, A. *Regenerative Medicine: Translational Approaches and Tissue Engineering*. Boston, MA: Artech House, 2007.
- Johnson, P.C., Mikos, A.G., Fisher, J.P., and Jansen, J.A. Strategic directions in tissue engineering. *Tissue Eng* **13**, 2827, 2007.
- Koning, M., Harmsen, M.C., van Luyn, M.J., and Werker, P.M. Current opportunities and challenges in skeletal muscle tissue engineering. *J Tissue Eng Regen Med* **3**, 407, 2009.
- Mikos, A.G., Herring, S.W., Ochareon, P., Elisseeff, J., Lu, H.H., Kandel, R., Schoen, F.J., Toner, M., Mooney, D., Atala, A., Van Dyke, M.E., Kaplan, D., and Vunjak-Novakovic, G. Engineering complex tissues. *Tissue Eng* **12**, 3307, 2006.
- Kuang, S., Gillespie, M.A., and Rudnicki, M.A. Niche regulation of muscle satellite cell self-renewal and differentiation. *Cell Stem Cell* **2**, 22, 2008.
- Meng, J., Muntoni, F., and Morgan, J.E. Stem cells to treat muscular dystrophies—Where are we? *Neuromuscul Disord* **21**, 4, 2011.
- Dezawa, M., Ishikawa, H., Itokazu, Y., Yoshihara, T., Hoshino, M., Takeda, S., Ide, C., and Nabeshima, Y. Bone marrow stromal cells generate muscle cells and repair muscle degeneration. *Science* **309**, 314, 2005.
- Wang, H.S., Hung, S.C., Peng, S.T., Huang, C.C., Wei, H.M., Guo, Y.J., Fu, Y.S., Lai, M.C., and Chen, C.C. Mesenchymal stem cells in the Wharton's jelly of the human umbilical cord. *Stem Cells* **22**, 1330, 2004.



9. Troyer, D.L., and Weiss, M.L. Wharton's jelly-derived cells are a primitive stromal cell population. *Stem Cells* **26**, 591, 2008.
10. Zhao, L., Weir, M.D., and Xu, H.H. An injectable calcium phosphate-alginate hydrogel-umbilical cord mesenchymal stem cell paste for bone tissue engineering. *Biomaterials* **31**, 6502, 2010.
11. Zhao, L., Weir, M.D., and Xu, H.H. Human umbilical cord stem cell encapsulation in calcium phosphate scaffolds for bone engineering. *Biomaterials* **31**, 3848, 2010.
12. Wang, L., Seshareddy, K., Weiss, M.L., and Detamore, M.S. Effect of initial seeding density on human umbilical cord mesenchymal stromal cells for fibrocartilage tissue engineering. *Tissue Eng Part A* **15**, 1009, 2009.
13. Wang, L., Tran, I., Seshareddy, K., Weiss, M.L., and Detamore, M.S. A comparison of human bone marrow-derived mesenchymal stem cells and human umbilical cord-derived mesenchymal stromal cells for cartilage tissue engineering. *Tissue Eng Part A* **15**, 2259, 2009.
14. Conconi, M.T., Burra, P., Di Liddo, R., Calore, C., Turetta, M., Bellini, S., Bo, P., Nussdorfer, G.G., and Parnigotto, P.P. CD105(+) cells from Wharton's jelly show *in vitro* and *in vivo* myogenic differentiative potential. *Int J Mol Med* **18**, 1089, 2006.
15. Kocafee, C., Balci, D., Hayta, B.B., and Can, A. Reprogramming of human umbilical cord stromal mesenchymal stem cells for myogenic differentiation and muscle repair. *Stem Cell Rev* **6**, 512, 2010.
16. Qian, Q., Qian, H., Zhang, X., Zhu, W., Yan, Y., Ye, S., Peng, X., Li, W., Xu, Z., Sun, L., and Xu, W. 5-Azacytidine induces cardiac differentiation of human umbilical cord derived mesenchymal stem cells by activating extracellular regulated kinase (ERK). *Stem Cells Dev* **21**, 67, 2012.
17. Kloxin, A.M., Kasko, A.M., Salinas, C.N., and Anseth, K.S. Photodegradable hydrogels for dynamic tuning of physical and chemical properties. *Science* **324**, 59, 2009.
18. Kretlow, J.D., Young, S., Klouda, L., Wong, M., and Mikos, A.G. Injectable biomaterials for regenerating complex craniofacial tissues. *Adv Mater* **21**, 3368, 2009.
19. Hill, E., Boontheekul, T., and Mooney, D.J. Designing scaffolds to enhance transplanted myoblast survival and migration. *Tissue Eng* **12**, 1295, 2006.
20. Rowley, J.A., Madlambayan, G., and Mooney, D.J. Alginate hydrogels as synthetic extracellular matrix materials. *Biomaterials* **20**, 45, 1999.
21. Boontheekul, T., Hill, E.E., Kong, H.J., and Mooney, D.J. Regulating myoblast phenotype through controlled gel stiffness and degradation. *Tissue Eng* **13**, 1431, 2007.
22. Huang, Y.C., Dennis, R.G., Larkin, L., and Baar, K. Rapid formation of functional muscle *in vitro* using fibrin gels. *J Appl Physiol* **98**, 706, 2005.
23. Kroehne, V., Heschel, I., Schugner, F., Lasrich, D., Bartsch, J.W., and Jockusch, H. Use of a novel collagen matrix with oriented pore structure for muscle cell differentiation in cell culture and in grafts. *J Cell Mol Med* **12**, 1640, 2008.
24. Varghese, S., and Elisseeff, J. Hydrogels for musculoskeletal tissue engineering. *Adv Polym Sci* **203**, 95, 2006.
25. Lee, K.Y., and Mooney, D.J. Hydrogels for tissue engineering. *Chem Rev* **101**, 1869, 2001.
26. Cushing, M.C., Liao, J.T., Jaeggli, M.P., and Anseth, K.S. Material-based regulation of the myofibroblast phenotype. *Biomaterials* **28**, 3378, 2007.
27. Zhou, H., and Xu, H.H.K. The fast release of stem cells from alginate-fibrin microbeads in injectable scaffolds for bone tissue engineering. *Biomaterials* **32**, 7503, 2011.
28. Chen, W., Zhou, H., Tang, M., Weir, M.D., Bao, C., and Xu, H.H.K. Gas-foaming calcium phosphate cement scaffold encapsulating human umbilical cord stem cells. *Tissue Eng Part A* **18**, 816, 2011.
29. Wakitani, S., Saito, T., and Caplan, A.I. Myogenic cells derived from rat bone marrow mesenchymal stem cells exposed to 5-azacytidine. *Muscle Nerve* **18**, 1417, 1995.
30. Makino, S., Fukuda, K., Miyoshi, S., Konishi, F., Kodama, H., Pan, J., Sano, M., Takahashi, T., Hori, S., Abe, H., Hata, J., Umezawa, A., and Ogawa, S. Cardiomyocytes can be generated from marrow stromal cells *in vitro*. *J Clin Invest* **103**, 697, 1999.
31. Rowley, J.A., and Mooney, D.J. Alginate type and RGD density control myoblast phenotype. *J Biomed Mater Res* **60**, 217, 2002.
32. Boontheekul, T., Kong, H.-J., and Mooney, D.J. Controlling alginate gel degradation utilizing partial oxidation and bimodal molecular weight distribution. *Biomaterials* **26**, 2455, 2005.
33. Bouhadir, K.H., Lee, K.Y., Alsborg, E., Damm, K.L., Anderson, K.W., and Mooney, D.J. Degradation of partially oxidized alginate and its potential application for tissue engineering. *Biotechnol Prog* **17**, 945, 2001.
34. Fragonas, E., Valente, M., Pozzi-Mucelli, M., Toffanin, R., Rizzo, R., Silvestri, F., and Vittur, F. Articular cartilage repair in rabbits by using suspensions of allogenic chondrocytes in alginate. *Biomaterials* **21**, 795, 2000.
35. Ahmed, N., Dreier, R., Gopferich, A., Grifka, J., and Grassel, S. Soluble signalling factors derived from differentiated cartilage tissue affect chondrogenic differentiation of rat adult marrow stromal cells. *Cell Physiol Biochem* **20**, 665, 2007.
36. Li, J., Zhao, Z., Yang, J., Liu, J., Wang, J., Li, X., and Liu, Y. p38 MAPK mediated in compressive stress-induced chondrogenesis of rat bone marrow MSCs in 3D alginate scaffolds. *J Cell Physiol* **221**, 609, 2009.
37. Re'em, T., Tsur-Gang, O., and Cohen, S. The effect of immobilized RGD peptide in macroporous alginate scaffolds on TGF $\beta$ 1-induced chondrogenesis of human mesenchymal stem cells. *Biomaterials* **31**, 6746, 2010.
38. Maguire, T., Davidovich, A.E., Wallenstein, E.J., Novik, E., Sharma, N., Pedersen, H., Androulakis, I.P., Schloss, R., and Yarmush, M. Control of hepatic differentiation via cellular aggregation in an alginate microenvironment. *Biotechnol Bioeng* **98**, 631, 2007.
39. Szasz, G., Gruber, W., and Bernt, E. Creatine kinase in serum: 1. Determination of optimum reaction conditions. *Clin Chem* **22**, 650, 1976.
40. van der Velden, J.L.J., Langen, R.C.J., Kelders, M.C., Wouters, E.F.M., Janssen-Heininger, Y.M.W., and Schols, A.M. Inhibition of glycogen synthase kinase-3 $\beta$  activity is sufficient to stimulate myogenic differentiation. *Am J Physiol Cell Physiol* **290**, C453, 2006.
41. Bradford, M.M. A rapid and sensitive method for the quantitation of microgram quantities of protein utilizing the principle of protein-dye binding. *Anal Biochem* **72**, 248, 1976.
42. Charge, S.B., and Rudnicki, M.A. Cellular and molecular regulation of muscle regeneration. *Physiol Rev* **84**, 209, 2004.
43. Dogra, C., Changotra, H., Mohan, S., and Kumar, A. Tumor necrosis factor-like weak inducer of apoptosis inhibits skeletal myogenesis through sustained activation of nuclear factor-kappaB and degradation of MyoD protein. *J Biol Chem* **281**, 10327, 2006.
44. Gorodetsky, R., Vexler, A., Leviansky, L., and Marx, G. Fibrin microbeads (FMB) as biodegradable carriers for cul-



- turing cells and for accelerating wound healing. *Methods Mol Biol* **238**, 11, 2004.
45. Marx, G., Mou, X., Hotovely-Salomon, A., Levdansky, L., Gaberman, E., Belenky, D., and Gorodetsky, R. Heat denaturation of fibrinogen to develop a biomedical matrix. *J Biomed Mater Res B Appl Biomater* **84**, 49, 2008.
  46. Perka, C., Arnold, U., Spitzer, R.S., and Lindenhayn, K. The use of fibrin beads for tissue engineering and subsequential transplantation. *Tissue Eng* **7**, 359, 2001.
  47. Simon, C.G., Jr., Guthrie, W.F., and Wang, F.W. Cell seeding into calcium phosphate cement. *J Biomed Mater Res A* **68**, 628, 2004.
  48. Weir, M.D., Xu, H.H., and Simon, C.G., Jr. Strong calcium phosphate cement-chitosan-mesh construct containing cell-encapsulating hydrogel beads for bone tissue engineering. *J Biomed Mater Res A* **77**, 487, 2006.
  49. Evangelista, M.B., Hsiong, S.X., Fernandes, R., Sampaio, P., Kong, H.-J., Barrias, C.C., Salema, R., Barbosa, M.A., Mooney, D.J., and Granja, P.L. Upregulation of bone cell differentiation through immobilization within a synthetic extracellular matrix. *Biomaterials* **28**, 3644, 2007.
  50. Hollister, S.J. Porous scaffold design for tissue engineering. *Nat Mater* **4**, 518, 2005.
  51. Radin, S., Chen, T., and Ducheyne, P. The controlled release of drugs from emulsified, sol gel processed silica microspheres. *Biomaterials* **30**, 850, 2009.
  52. Silva, G.A., Coutinho, O.P., and Ducheyne, P., Reis, R.L. Materials in particulate form for tissue engineering. 2. Applications in bone. *J Tissue Eng Regen Med* **1**, 97, 2007.
  53. Eiselt, P., Yeh, J., Latvala, R.K., Shea, L.D., and Mooney, D.J. Porous carriers for biomedical applications based on alginate hydrogels. *Biomaterials* **21**, 1921, 2000.
  54. Smidsrod, O., and Skjak-Braek, G. Alginate as immobilization matrix for cells. *Trends Biotechnol* **8**, 71, 1990.
  55. Shachar, M., Tsur-Gang, O., Dvir, T., Leor, J., and Cohen, S. The effect of immobilized RGD peptide in alginate scaffolds on cardiac tissue engineering. *Acta Biomater* **7**, 152, 2011.
  56. Hwang, C.M., Sant, S., Masaeli, M., Kachouie, N.N., Zamanian, B., Lee, S.H., and Khademhosseini, A. Fabrication of three-dimensional porous cell-laden hydrogel for tissue engineering. *Biofabrication* **2**, 035003, 2010.
  57. Ahmed, T.A., Dare, E.V., and Hincke, M. Fibrin: a versatile scaffold for tissue engineering applications. *Tissue Eng Part B* **14**, 199, 2008.
  58. Yang, Y., Palmer, K.C., Relan, N., Diglio, C., and Schuger, L. Role of laminin polymerization at the epithelial mesenchymal interface in bronchial myogenesis. *Development* **125**, 2621, 1998.
  59. Relan, N.K., Yang, Y., Beqaj, S., Miner, J.H., and Schuger, L. Cell elongation induces laminin  $\alpha 2$  chain expression in mouse embryonic mesenchymal cells: role in visceral myogenesis. *J Cell Biol* **147**, 1341, 1999.
  60. Huebsch, N., Arany, P.R., Mao, A.S., Shvartsman, D., Ali, O.A., Bencherif, S.A., *et al.* Harnessing traction-mediated manipulation of the cell/matrix interface to control stem-cell fate. *Nat Mater* **9**, 518, 2010.
  61. Tibbitt, M.W., and Anseth, K.S. Hydrogels as extracellular matrix mimics for 3D cell culture. *Biotechnol Bioeng* **103**, 655, 2009.
  62. Matsuki, K., Sasho, T., Nakagawa, K., Tahara, M., Sugioka, K., Ochiai, N., Ogino, S., Wada, Y., and Moriya, H. RGD peptide-induced cell death of chondrocytes and synovial cells. *J Orthop Sci* **13**, 524, 2008.
  63. Ruoslahti, E., and Pierschbacher, M.D. New perspectives in cell adhesion: RGD and integrins. *Science* **238**, 491, 1987.
  64. Simon, C.G., Jr., and Lin-Gibson, S. Combinatorial and high-throughput screening of biomaterials. *Adv Mater* **23**, 369, 2011.
  65. Morgan, A.W., Roskov, K.E., Lin-Gibson, S., Kaplan, D.L., Becker, M.L., and Simon Jr, C.G. Characterization and optimization of RGD-containing silk blends to support osteoblastic differentiation. *Biomaterials* **29**, 2556, 2008.
  66. Hersel, U., Dahmen, C., and Kessler, H. RGD modified polymers: biomaterials for stimulated cell adhesion and beyond. *Biomaterials* **24**, 4385, 2003.
  67. Trotman, C.A., Faraway, J.J., Phillips, C., and van Aalst, J. Effects of lip revision surgery in cleft lip/palate patients. *J Dent Res* **89**, 728, 2010.
  68. Trotman, C.A., Faraway, J.J., Losken, H.W., and van Aalst, J.A. Functional outcomes of cleft lip surgery. Part II: quantification of nasolabial movement. *Cleft Palate Craniofac J* **44**, 607, 2007.
  69. Trotman, C.A., Faraway, J.J., and Essick, G.K. Three-dimensional nasolabial displacement during movement in repaired cleft lip and palate patients. *Plast Reconstr Surg* **105**, 1273, 2000.

Address correspondence to:

Hockin H. K. Xu, Ph.D.

*Biomaterials and Tissue Engineering Division*

*Department of Endodontics*

*University of Maryland Dental School*

*650 West Baltimore Street*

*Baltimore, MD 21201*

*E-mail: hxu@umaryland.edu*

Qiangming Chen, D.D.S., Ph.D.

*State Key Laboratory of Oral Diseases*

*West China School of Stomatology*

*Sichuan University*

*No. 14, 3rd Section, RenMinNan Road*

*Chengdu 610041*

*China*

*E-mail: qmchen@scu.edu.cn*

Carroll Ann Trotman, B.D.S., M.A., M.S.

*University of Maryland Dental School*

*650 West Baltimore Street*

*Baltimore, MD 21201*

*E-mail: ctrotman@umaryland.edu*

*Received: December 12, 2011*

*Accepted: June 11, 2012*

*Online Publication Date: July 18, 2012*